

# Direct Covalent Attachment of DNA Microarrays by Rapid Thiol–Ene “Click” Chemistry

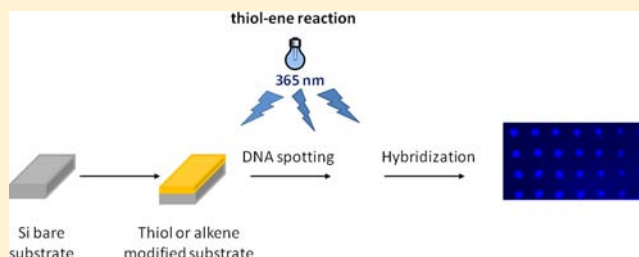
Jorge Escorihuela,<sup>†</sup> María-José Bañuls,<sup>†</sup> Santiago Grijalvo,<sup>‡</sup> Ramón Eritja,<sup>‡</sup> Rosa Puchades,<sup>†</sup> and Àngel Maquieira<sup>\*,†</sup>

<sup>†</sup>Centro de Reconocimiento Molecular y Desarrollo Tecnológico, Departamento de Química, Universitat Politècnica de València, Camino de Vera s/n, 46022 Valencia, Spain

<sup>‡</sup>Networking Center on Bioengineering, Biomaterials and Biomedicine (CIBER-BBN) and Institute for Advanced Chemistry of Catalonia (IQAC-CSIC), Chemical and Biomolecular Nanotechnology Department, Jordi Girona 18-26, 08034 Barcelona, Spain

## Supporting Information

**ABSTRACT:** A rapid strategy for the covalent immobilization of DNA onto silicon-based materials using the UV-initiated radical thiol–ene reaction is presented in this study. Following this approach, thiol- and alkene-modified oligonucleotide probes were covalently attached in microarray format, reaching immobilization densities around  $6 \text{ pmol}\cdot\text{cm}^{-2}$ . The developed methodology presents the advantages of spatially controlled probe anchoring (using a photomask), direct attachment without using cross-linkers (one-pot fashion), and short irradiation times (20 min). Using the described strategy, hybridization efficiencies up to 65% with full complementary strands were reached. The approach was evaluated by scoring single-base pair mismatches with discrimination ratios around 15. Moreover, the efficacy of the proposed DNA detection scheme is further demonstrated through the assay on a genomic target of bacterial *Escherichia coli*.



## INTRODUCTION

Array technology monitors the interaction of a set of molecules, such as nucleic acids and proteins, with a predetermined library of molecular probes.<sup>1</sup> In the development of a useful and reliable chemistry for producing DNA arrays, the accessibility and functionality of the surface-bound probe, the density of immobilization, the reproducibility and stability of the attachment chemistry, and the fidelity of the anchored sequences are all critical parameters to be considered. In this regard, the development of efficient surface chemistries to modify the physical and chemical properties of supports has become essential to develop DNA chip technology.<sup>2</sup> Thus, different attachment methodologies have been implemented to anchor probes to solid substrates.<sup>3</sup> Typical methods involve the generation of active functional groups on the surface that react with an appropriately modified DNA probe. In this regard, organosilane compounds have been widely used in the surface modification of many materials and devices.<sup>4–9</sup>

The site-specific immobilization of biological ligands at well-defined locations on substrates is essentially required for certain biological assays,<sup>10,11</sup> for combinatorial screening, and for the fabrication of biosensors.<sup>12</sup> It is therefore of great interest to develop strategies that perform bioassays through robust and efficient chemical methodologies for the realization of DNA chip technology. As a result of its orthogonality and the ability to selectively pattern surfaces simply by simple exposure to UV light, thiol–ene chemistry has recently received increasing interest as a promising surface modification reaction.<sup>13,14</sup> The

thiol–ene reaction, which takes place with UV radiation and forms a thioether bond, is compatible with aqueous media chemistry, which is crucial for its bioutilty.<sup>15,16</sup> Thiol–ene reactions proceed under mild conditions in the presence of oxygen, are regioselective, tolerate many functional groups, can be performed on neat or in benign solvents such as water, and provide quantitative or near-quantitative yields. Although many of the initial uses of thiol–ene chemistry focused on photocurable polymers and resins for its use in protective coatings and films,<sup>17,18</sup> this novel click reaction has proven to be an elegant and facile method to anchor biomolecules to silicon-based surfaces.<sup>19–28</sup> The reported methods generally employ silane coupling agents and need a further reaction with different secondary polymers or cross-linking reagents to provide covalent anchoring of probes.

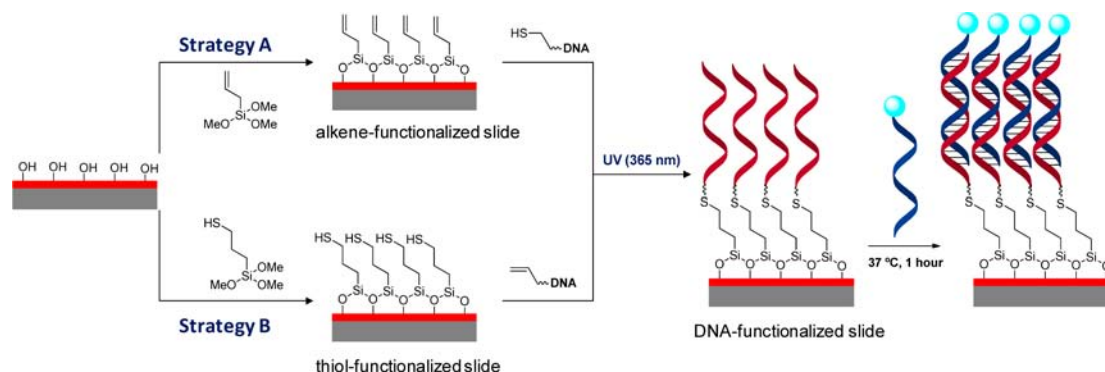
In a recent work, we reported on the use of thiol–ene “click” chemistry for the covalent immobilization of a biotin-derivative to a silicon based surface, and then, we immobilized biotin-functionalized oligonucleotides through a streptavidin bridge.<sup>26</sup> This approach constituted a selective strategy to prepare DNA microarrays and allowed the discrimination of genetic variations. However, covalent attachment of DNA probes is normally preferred because of its robustness and reproducibility. In this regard, the search for new methodologies to

**Received:** January 24, 2014

**Revised:** February 20, 2014

**Published:** February 21, 2014

Scheme 1. Thiol–ene Reaction for the Immobilization of Oligonucleotides<sup>a</sup>



<sup>a</sup>Surfaces were functionalized with allyltrimethoxysilane (Strategy A) and 3-mercaptopropyl trimethoxysilane (Strategy B).

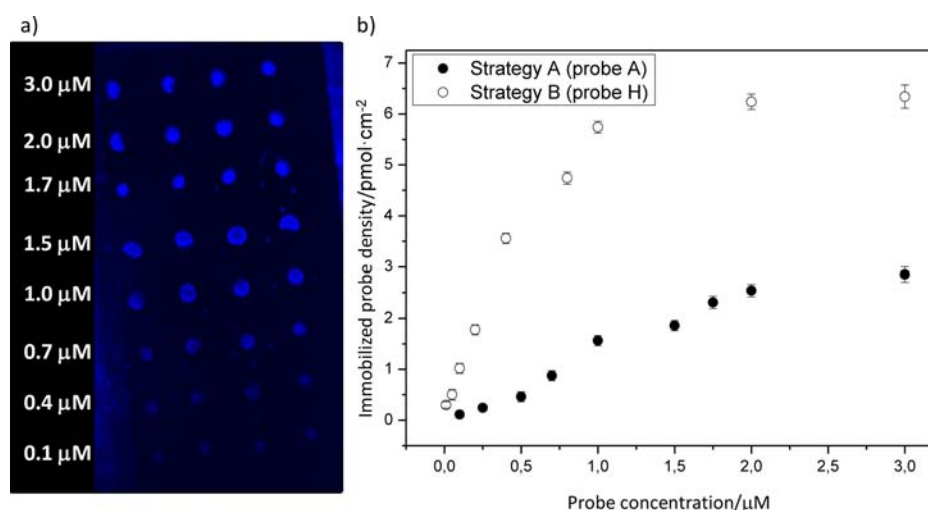


**Figure 1.** (a) Fluorescence image of an array of probes immobilized at different concentrations and (b) oligonucleotide immobilization density for probes A (Strategy A) and H (Strategy B).

covalently attach oligonucleotides to solid supports has emerged as a hot topic in chemistry and materials science.

Herein, we report for the first time a simple and rapid strategy to covalently bind DNA oligonucleotides on silicon-based substrates using the thiol–ene reaction, without the use of intermediate reagents or cross-linkers. We demonstrate the potential application of this approach by preparing locally DNA functionalized surfaces and developing hybridization assays which allow effective discrimination of base mismatch. Also, for the first time, a DNA microarray created using the thiol–ene reaction is used for real samples and bacterial *Escherichia coli* is specifically detected.

## RESULTS AND DISCUSSION

**Immobilization Assays.** To adopt the thiol–ene reaction for the immobilization of oligonucleotides, surfaces were functionalized with allyltrimethoxysilane (strategy A) and 3-mercaptopropyl trimethoxysilane (strategy B). For that, silicon-oxide-coated silicon slides were chosen as starting material, cleaned with piranha solution, and subsequently functionalized with the appropriate organosilane compound (2% in toluene). When investigating the silanization time by means of water contact angle (WCA) measurements, a rapid increase in the hydrophobicity was initially observed during the first 10 min, followed by a slight variation in the first 2 h, which remained

essentially constant after 4 h. According to this, the silanization time was set at 2 h. The silanization reaction was also investigated in different solvents, but no significant differences were observed when evaluating the surface wettability.

For the performance of the proposed strategies (Scheme 1), commercially available thiol-modified oligonucleotides were used. With strategy B, a set of alkene 5'-terminated oligonucleotide probes were synthesized (probes H–L). In these cases, a spacer was introduced in order to have a suitable separation between the silicon surface and the oligonucleotide probes. For that, a hydrophilic spacer, monoallyl-tetraethylene glycol, was derivatized to its corresponding phosphoramidite (see Supporting Information) and was covalently linked into several oligonucleotide probes with excellent coupling yields (>90%) at their 5'-termini (5'-alkene-modified probes).

Next, the covalent anchoring of Cy5-labeled oligonucleotides through thiol–ene chemistry was investigated. Probe A was used for the photoimmobilization on alkene-functionalized surfaces (Strategy A), whereas the synthesized alkene-probe H was anchored onto the thiol-modified surfaces (Strategy B). For that purpose, slides were functionalized with allyltrimethoxysilane or 3-mercaptopropyl trimethoxysilane under the described conditions to obtain the alkene- or thiol-functionalized surfaces, respectively. Then, probes A and H were drop cast onto the functionalized slides and exposed to UV-light (365 nm) to induce the photoimmobilization. After exposure

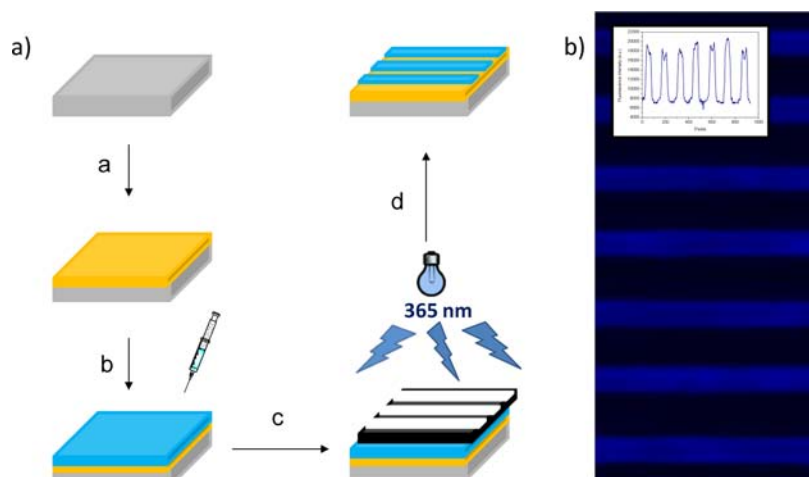


**Figure 2.** (A) Schematic illustration of the surface patterning. Surface modification: (a) silanization; (b) drop casting of Cy5-labeled DNA; (c) irradiation through a photomask; (d) removal of the photomask and washings. (B) Fluorescence image obtained after irradiation through a photomask.

and washing, fluorescence was measured with a surface fluorescence reader (see Supporting Information).

Initially, the influence of several parameters, such as time and pH, was studied. In this regard, no significant differences on the immobilization were observed for the pH range under study (buffers with different pH from 4 to 12). Additionally, the grafting of probes was investigated at different irradiation times. To this end, probe A (2  $\mu\text{M}$ ) was spotted and incubated at different times. After washing the slides, low signal-to-noise ratios (S/N) were obtained for short times. Better immobilization efficiencies and S/N ratios were achieved for longer times, with maximum values accomplished after 20 min (see Supporting Information). Negligible responses ( $\text{S/N} < 3$ ) were obtained from a noncovalent probe anchoring on functionalized surfaces when fluorescent labeled oligonucleotides without thiol (Strategy A) or alkene group (Strategy B) were used, following strategies A or B, respectively. Furthermore, when working with either unmodified silicon or surfaces modified with triethoxymethylsilane, no fluorescence of the Cy5-labeled probe was detected after exposure to UV-light and washings, suggesting a poor nonspecific interaction of probe DNA.

A quantitative analysis of the immobilization efficiency was performed using a standard calibration curve, plotting fluorescence intensity and amount of spotted probe (see Supporting Information). For that, probes A and H were serially diluted to a range of concentrations (0.05 to 3  $\mu\text{M}$ ) and spotted onto the functionalized slides, and after irradiation and washing, the fluorescence of the spots was analyzed (Figure 1a). As shown in Figure 1b, a surface coverage around 3 and 6  $\text{pmol}\cdot\text{cm}^{-2}$  was reached for strategies A and B, respectively. The obtained densities were similar to those reported by other authors who work on distinct substrates.<sup>29,30</sup> The differences in the immobilization density can be rationalized by means of the mechanism for DNA probe immobilization by the thiol–ene reaction. In this regard, for strategy A, thiol radicals were generated by UV irradiation in the solution media; hence, thiolated probes may react among them to form disulfide bonds,<sup>31</sup> which inhibit the covalent attachment to the surface, subsequently lowering the surface coverage. This radical quenching was not favored in strategy B, where thiol radicals were covalently attached to the surface. To study the effect of

the 15 T spacer arm on the immobilization yield, immobilization studies were done with probe M (containing the same sequence as probe A but lacking the poly T tail). The results revealed a similar immobilization density to that observed for probe A (2.7  $\text{pmol}\cdot\text{cm}^{-2}$ ), indicating poor spacer influence in the anchoring step.

It is noteworthy that high immobilization densities do not necessarily imply an improvement in the hybridization efficiency, so these immobilization results make the strategy suitable to detect DNA with high sensitivities.<sup>32</sup> In both cases, the immobilization densities increased with the dispensed oligonucleotide concentration, reaching a plateau at concentrations around 2  $\mu\text{M}$ . Interestingly, when interchip reproducibility was studied, a standard deviation below 12% was obtained for measurements on different days, which shows the robustness of the described immobilization approach.

Photolithography, which is commonly used in microfabrication processes, has been recently adapted to construct microarrays of proteins,<sup>33,34</sup> polymers,<sup>35</sup> and oligonucleotides.<sup>36</sup> The use of this approach to construct patterned surfaces is essentially accomplished by using contact photomasks. As shown in Figure 2, we patterned the distribution of probe A onto an alkene-modified surface by selective irradiation at 365 nm through a photomask for 20 min. Subsequent washings removed unbound molecules and led to the patterning of covalently attached oligonucleotides. These results indicate that the covalent attachment of oligonucleotides to the surface occurs specifically through the proposed thiol–ene reaction. The homogeneity and well-defined distribution of the fluorescent DNA motifs displays the efficiency of the coupling reaction and, consequently, the high density of the Cy5-labeled DNA anchored on the organosilane monolayer and its potential use in material sciences.

**Surface Characterization.** The chemical functionalization of the surface was investigated by employing different surface characterization techniques. After cleaning with piranha solution, the contact angle was below  $10^\circ$ , indicating that the hydroxylated  $\text{SiO}_2$  surface was very hydrophilic. Upon reaction with allyltrimethoxysilane, the WCA increased to  $84^\circ$  (see Supporting Information), which is in accordance with the presence of a more hydrophobic layer on the surface. Finally, after the immobilization of DNA probe by UV irradiation, the

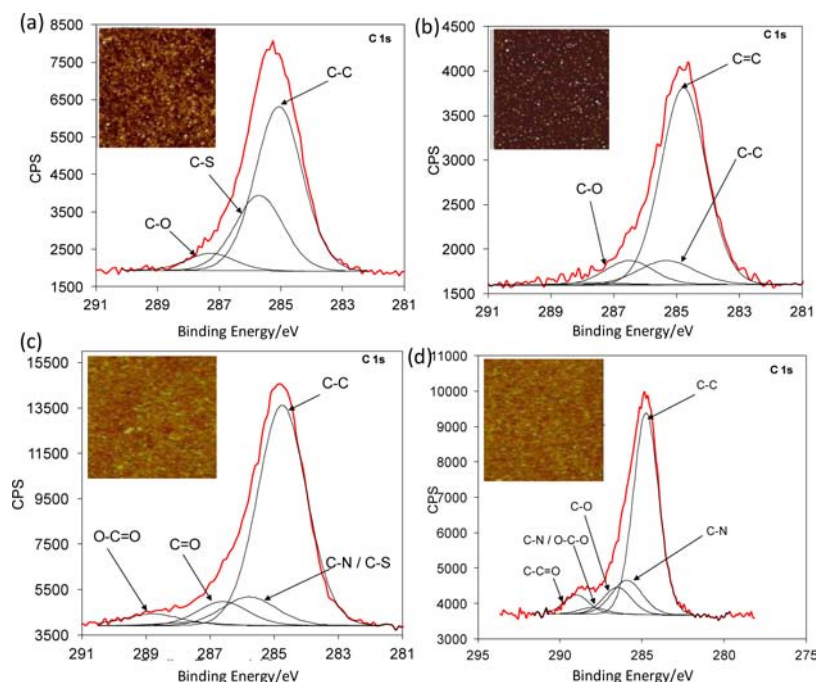


**Figure 3.** C 1s XPS spectra of: alkene (A), thiol (B), and DNA-functionalized slides following strategies A (C) or B (D). Inset: AFM images ( $2 \times 2 \mu\text{m}$ ).

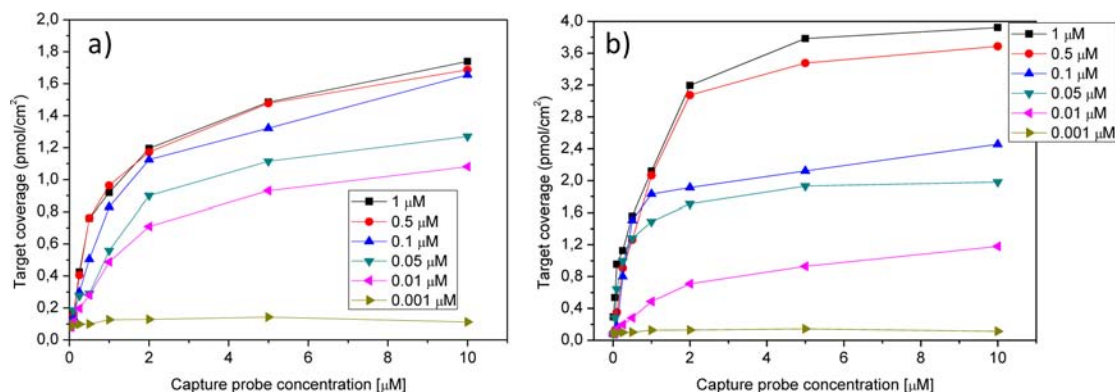


**Figure 4.** Hybridized target density for different capture probe concentrations: (a) Probe B, target A (Strategy A) and (b) Probe I, target B (Strategy B).

WCA decreased to  $51^\circ$ , as observed for similar systems ( $50^\circ$  for DNA immobilization on other Si surfaces).<sup>37</sup> For the thiolated surface used in strategy B, a WCA of  $58^\circ$  was measured after organosilanization, whereas after DNA probe attachment dropped to  $53^\circ$ , which was similar to the value obtained for strategy A.

Evidence for the viability of the thiol-ene chemistry employed for oligonucleotide immobilization was also obtained by XPS and IRRAS analyses (see Supporting Information). From the XPS analysis, organosilane attachment to the  $\text{SiO}_2$  wafer resulted in a decrease in the Si signal and an increase in the C 1s signal as compared to the raw material. The narrow scan of C 1s signal was used to probe the chemical states of carbon on the surface (Figure 3). All the electron binding energies of the different types of carbon peak positions were derived from the literature.<sup>38</sup> For the alkene-functionalized surfaces, the C 1s signal can be deconvoluted into three components at 286.5, 285.3, and 284.9 eV, respectively assigned to C-O, C-C, and C=C carbon atoms. The IRRAS spectrum of the alkene-modified surface exhibited alkyl

$\text{CH}_2$  stretch bands at 2932 and 2864  $\text{cm}^{-1}$ . Moreover, a band at 3082  $\text{cm}^{-1}$  corresponding to allyl C-H was also observed. For the thiol-functionalized surface, the C 1s signal can be deconvoluted into three components at 287, 286, and 285 eV, respectively, assigned to C-O, C-S, and C-C carbon atoms. Bands corresponding to the characteristic stretching vibrations of H-C-H (2932 and 2864  $\text{cm}^{-1}$ ) and thiol S-H stretch (2571  $\text{cm}^{-1}$ ) were observed in the IRRAS spectrum. For the DNA-functionalized surface, the C 1s spectrum was decomposed into four different carbon positions, assigned to C-O, C-S, and C-C carbon atoms, and another new band at 288.8 eV corresponding to C=O carbon atom (Figure 4), which represent the carbon species specific to the DNA bases.<sup>39,40</sup> The XPS data also show the attachment of DNA on the surface with a strong peak in the N 1s region and an increase in the intensity of the C 1s peak at 288 eV, characteristic of carbons associated with electron withdrawing groups such as nitrogen and oxygen. The reaction of the alkene-terminated surface with the thiolated oligonucleotide lead to an increase of the H-C-H stretch bands and the



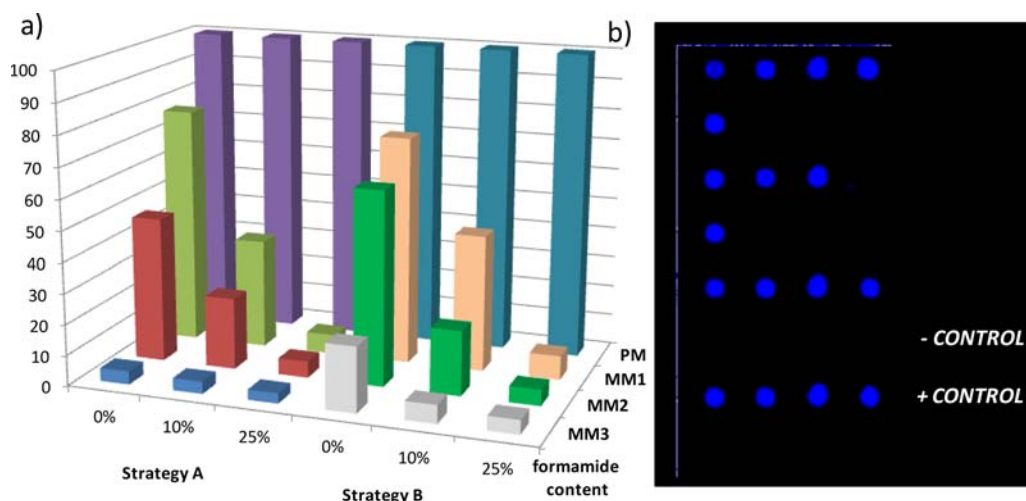


**Figure 5.** (a) Effect of formamide in the SNPs detection (PM: perfect match; MM1: 1 mismatch; MM2: 2 mismatches; MM3: 3 mismatches). (b) Specific detection of bacterial *E. coli*.

disappearance of the vinyl C–H signal, as observed in the IRRAS spectrum.

The topography of the different functionalized surfaces was analyzed by AFM (Figure 3 inset). Unmodified Si wafers were relatively flat, as inferred from the root-mean-square (rms) roughness value over the  $2 \times 2 \mu\text{m}^2$  regions for the clean  $\text{SiO}_2$  (1.64 nm). Interestingly, after reaction with the organosilane, roughness increased to 2.10 and 2.37 nm for the alkene- or thiol-functionalized surfaces, respectively. The ellipsometric thicknesses of the alkene- or thiol-functionalized surfaces were  $1.0 \pm 0.2$  and  $1.3 \pm 0.3$  nm, respectively. These data indicate the presence of a silane monolayer on the silicon surface. Remarkably, after DNA immobilization, rms increased to 3.47 nm, indicating the effective coverage of oligonucleotide probe to the surface.<sup>41,42</sup> Similar values of thicknesses after DNA attachment were observed for both strategies (around 3.3 nm), which support that the DNA probe is immobilized in a “flat” disposition.

**Hybridization Assays.** The applicability of the proposed methodology to attach DNA probes was assessed through hybridization assays with oligonucleotides and PCR products, establishing its sensitivity and selectivity. For that, 5'-thiol-modified probe B (Strategy A) and 5'-alkene-modified probe I (Strategy B) were spotted onto the functionalized slides following the described procedures. After irradiation and washings, Cy5-labeled complementary oligonucleotide in the hybridization buffer was dispensed, incubated, and, after rinsing and drying, the fluorescence intensity was registered. Initially, the hybridization conditions were optimized and the influence of parameters, such as time and temperature of hybridization, were studied. From the data (see Supporting Information), best results in terms of fluorescence intensity were obtained when performing the hybridization at 37 °C for 1 h.

Next, the performance of DNA microarray was further characterized by comparing hybridization sensitivity at different capture probe (0.05 to 10  $\mu\text{M}$ ) and target concentrations (0.001 to 1  $\mu\text{M}$ ). Hybridization signal intensities diminished at lower probe (0.05 to 1  $\mu\text{M}$ ) concentrations, indicating the effects of immobilized probe density on hybridization efficiency. The amount of hybridized DNA was interpolated from the corresponding calibration curves, reaching maximum values of 1.8 and 3.9  $\text{pmol}\cdot\text{cm}^{-2}$  for strategy A and B, respectively

(Figure 4). These densities are in accordance with the different amount of immobilized probe in the two strategies and they correspond to hybridization yields of 60% and 65%. Control experiments on surfaces without immobilized probes were performed and nonspecific adsorption of DNA targets on the thiol or alkene-functionalized surfaces was not observed.

The calculated limit of detection was on the order of 100 pM, estimated as the concentration that gives a fluorescence signal three times the standard deviation of the signal obtained with a noncomplementary strand. This detection limit is similar to that obtained for fluorescence arrays on other surfaces.<sup>43</sup> To determine the intrachip and chip-to-chip relative standard deviations, the signals obtained after the analysis of PCR products corresponding to 100 nM were analyzed. The intrachip RSD varied from 7% to 10%, whereas it ranged from 8% to 12% for the chip-to-chip RSD. These results corroborate the good performances of the arrays to detect genomic DNA at very low levels. It is noteworthy that, unlike the majority of the reported methods in DNA microarrays,<sup>44</sup> a blocking step was not needed to achieve these results, thus providing the advantages of simplifying and reducing the time required to perform the assay.

The ability to differentiate single base mismatches has been the hallmark of the selectivity associated with a DNA assay.<sup>45,46</sup> In order to demonstrate the selectivity of the proposed strategy, a base mismatch study was carried out by immobilizing five 5'-SH-modified probes (containing zero to three mismatches and a noncomplementary) onto alkene-functionalized silicon slides. After the usual processing, the slide was subjected to hybridization with a labeled complementary target (complementary to MM). After washings and drying, the chip was analyzed and the results revealed that spots corresponding to the perfectly matched probe displayed the highest fluorescence, while the single mismatched-probe (MM1) exhibited significantly low fluorescence and the spots corresponding to noncomplementary probe displayed no significant fluorescent (Figure 5a). However, the use of stringency conditions (ionic strength and formamide) allowed efficient discrimination of nucleotide with one single mismatch. Similar trends were observed for SNP discrimination assays using strategy B.

In order to gain more information about the hybridization process, both strategies were analyzed by dual-polarization

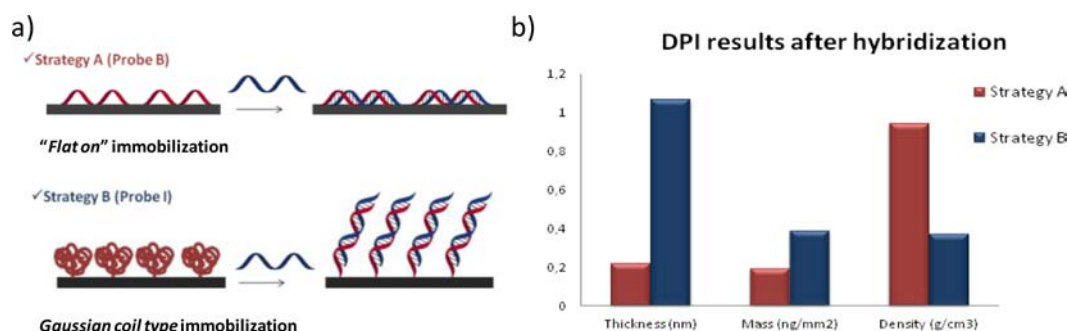


**Figure 6.** (a) Proposed models for the immobilization of probes and hybridization in strategies A and B. (b) Comparison of the values of thickness (nm), mass (ng/mm<sup>2</sup>), and density (g/cm<sup>3</sup>) obtained with DPI.

interferometry (DPI).<sup>47–49</sup> For that purpose, silicon oxynitride chips were functionalized with oligonucleotide probes following the described strategies (see Supporting Information). DPI data corroborated the results obtained in the microarray format and allowed us to establish a model to explain the hybridization process on the basis of different immobilization modes (Figure 6). For strategy A, a surface mass after hybridization of 0.19 ng·mm<sup>−2</sup> was observed, which corresponds to 2.8 pmol·cm<sup>−2</sup>. This means yielding hybridization efficiency of around 92% according to the maximum amount of immobilized probe. The layer thickness after hybridization remained almost unchanged, while the density increased considerably. These values may indicate that the probe is immobilized in a “flat on” conformation on the surface, and the hybridization takes place horizontally. This is also supported by ellipsometry measurements that reported a thickness increase of  $1.87 \pm 1.44$  nm after hybridization. For strategy B, the mass surface was 2-fold that observed for strategy A, yielding a similar hybridization efficiency when related to the maximum amount of immobilized probe. However, in this case the layer thickness increased 1 nm on average (which corresponds to 6.7 nm/molecule when considering the surface coverage referred to a close packed monolayer of dsDNA), while the increase in density was lower. This finding is in accordance with a Gaussian coil type immobilization for the alkene-probe, as described elsewhere.<sup>50</sup> Then, when the hybridization takes place, the coil is straightened out to produce a significant increase in layer thickness, but density lower in comparison to strategy A. Again, ellipsometry measurements were in agreement with the proposed immobilization model, as a thickness increase of  $9.45 \pm 1.83$  nm was observed after hybridization. In order to rule out the possible effect of the poly T spacer in the hybridization process, a similar study was done using probe M (Table 1). The results confirmed the poor influence of this spacer, as similar results were obtained when comparing probe B and M. The distinct immobilization modes postulated for both strategies might be attributed to the different nature of the surfaces, as corroborated by the measured contact angle values.

Finally, as a proof of concept, the potential of the new microarray for the sensitive and selective detection of PCR amplified DNA products of pathogens was tested (Figure 5b). The nucleotide sequence of the immobilized probe F was complementary to the central region of a specific amplicon to detect *E. coli*. Under the described conditions, the microarray was able to detect 50 pM of amplicon, which is lower than the limit of detection reached with synthetic oligonucleotides, and is probably due to the lower diffusion coefficient of larger targets.

**Table 1.** Nucleotide Sequence of Probes and Targets Used

Name	Sequence (5' to 3')	5' end	3' end
Probe A	(T) <sub>15</sub> -CCCGATTGACCAGCTAGCATT	SH	Cy5
Probe B	(T) <sub>15</sub> -CCCGATTGACCAGCTAGCATT	SH	----
Probe C	(T) <sub>15</sub> -CCCGATTGACCTGCTAGCATT	SH	----
Probe D	(T) <sub>15</sub> -CCCGATTGACTTGTAGCATT	SH	----
Probe E	(T) <sub>15</sub> -CCATATTGACCAGCTATCATT	SH	----
Probe F	(T) <sub>15</sub> -CGCCGATAACTCTGTCTCTGTA	SH	----
Probe G	(T) <sub>15</sub> -TCACGCCGATAACTCTGTCTCT	SH	----
Probe H	TTGATTACAGCCGGTGTACGACCCT	alkene	Cy5
Probe I	TTGATTACAGCCGGTGTACGACCCT	alkene	----
Probe J	TTGATTACAGCCGATGTACGACCCT	alkene	----
Probe K	TTGATTACAGCATGTGTACGACCCT	alkene	----
Probe L	TTGAACACAGCCGGTGTACGTCCT	alkene	----
Probe M	CCCGATTGACCAGCTAGCATT	SH	----
Target A	AATGCTAGCTGGTCAATCGGG	----	Cy5
Target B	AGGGTCACACCGGCTGTAATCAAA	----	Cy5

## CONCLUSIONS

In conclusion, a new and direct covalent attachment of oligonucleotides by thiol–ene chemistry on silicon-based surfaces has been developed to efficiently detect DNA. The reported immobilization methodology is fast, clean, and compatible with aqueous media chemistry, which is crucial for its bioutilility. The proposed approach allowed the covalent immobilization of modified probes with good densities to perform sensitive DNA hybridization assays. Detection of PCR amplified DNA products was also demonstrated, and reach high sensitivity and selectivity. Moreover, the limits of detection are very low and comparable to those reported in the literature using fluorescent, enzymatic, or metal nanoparticle labels on different supports. We also demonstrate that the performance achieved when employing the thiol on the surface and the alkene in the anchored probe improves the results obtained when using the alkenylated surface and thiol-ended probes. Furthermore, a probe immobilization model for both strategies based on dual polarization interferometry data is proposed. Finally, the described methodology may be very useful in the design and development of new DNA biosensors, and thus, the concept and strategy reported herein can also be applied to construct molecular nanodevices and point-of-care diagnosis.

## ■ EXPERIMENTAL SECTION

**Chemicals, Reagents, and Buffers.** *General.* The silicon-based wafers were provided by the Valencia Nanophotonics Technology Center (NTC) at the Universitat Politècnica de València (Spain) as 2- $\mu$ m-thick silicon oxide layer grown on (100) silicon wafer. Hydrogen peroxide (35% w/w), allyltrimethoxysilane, triethoxymethylsilane, 3-mercaptopropyl trimethoxysilane, and tetraethyleneglycol were purchased from Sigma-Aldrich Química (Madrid, Spain). Toluene, 2-propanol, and sulfuric acid 95–98% were purchased from Scharlau (Madrid, Spain). Note: All the chemicals should be handled by following the corresponding material safety data sheets. Milli-Q water with a resistivity above 18 m $\Omega$  was used to prepare aqueous solutions. The buffers employed were phosphate buffer saline (1  $\times$  PBS, 0.008 M sodium phosphate dibasic, 0.002 M sodium phosphate monobasic, 0.137 M sodium chloride, 0.003 M potassium chloride, pH 7.5), PBS-T (10 $\times$  PBS containing 0.05% Tween 20), and saline sodium citrate (1 $\times$  SSC, 0.15 M sodium chloride, 0.02 M sodium citrate, pH 7). All the solutions were filtered through a 0.22  $\mu$ m pore size nitrocellulose membrane from Whatman GmbH (Dassel, Germany) before use.

Unmodified, Cy5-labeled, and thiolated oligonucleotide sequences (probes A–G and M and targets A and B, Table 1) were acquired from Aldrich Química (Madrid, Spain). Alkene-modified oligonucleotides (probes H–L, Table 1) were synthesized. For the synthesis of these last oligonucleotide probes, all standard phosphoramidites used were purchased from Link Technologies. The benzoyl (Bz) group was used for the protection of the amino group of C and A, and the isobutryl (iBu) group for the protection of probe G. In all cases, the coupling yields were above 97%. Modified oligonucleotide probes were treated with aqueous concentrated ammonia at 55  $^{\circ}$ C overnight to cleave the products from the supports and remove the Bz and iBu groups. The resulting samples were filtered and ammonia solutions were concentrated to dryness. Oligonucleotides were desalted with Sephadex G-25 (NAP-10 column) and purified by semipreparative HPLC (see purification conditions below). DNA concentration and quality were determined by measuring the optical density at 260/280 nm with a NanoDrop ND 1000 Spectrophotometer (Thermo Fisher Scientific, Wilmington, Delaware).

**Instrumental Methods.** Microarray printing was carried out with a low volume noncontact dispensing system from Biodot (Irvine, CA, USA), model AD1500. Contact angle system OCA20 equipped with SCA20 software was from Dataphysics Instruments GmbH (Filderstadt, Germany). The measurements were done in quintuplicate at room temperature with a volume drop of 5  $\mu$ L employing 18 m $\Omega$  water quality. X-ray photoelectron spectra were recorded with a Sage 150 spectrophotometer from SPECS Surface Nano Analysis GmbH (Berlin, Germany). Non-monochromatic Al K $\alpha$  radiation (1486.6 eV) was used as the X-ray source operating at 30 eV constant pass energy for elemental specific energy binding analysis. Vacuum in the spectrometer chamber was 9  $\times$  10 $^{-9}$  hPa and the sample area analyzed was 1 mm $^2$ . Atomic force microscopy (AFM) images were obtained with a Veeco model Dimension 3100 Nanoman from Veeco Metrology (Santa Barbara, CA) using tapping mode at 300 kHz. Imaging was performed in AC mode in air using OMCL-AC240 silicon cantilevers (Olympus Corporation, Japan). The images were

captured using tips from Nano World with a radius of 8 nm. IRRAS spectra were recorded on a Bruker Tensor 27 FT-IR spectrometer using a commercial variable angle reflection unit (Auto Seagull, Harrick Scientific). All spectra were obtained at an incident angle of 68 $^{\circ}$  with 2048 scans recorded for each sample. The fluorescence signal of the spots was registered with a homemade surface fluorescence reader (SFR) having a high sensitivity charge coupled device camera Retiga EXi from Qimaging, Inc. (Burnaby, Canada), with light emitting diodes Toshiba TLOH157P as light source.<sup>51</sup> For microarray image analysis and subsequent quantification, GenePix Pro 4.0 software from Molecular Devices, Inc. (Sunnyvale, CA, USA), was employed.  $^1\text{H}$ ,  $^{13}\text{C}$ , and  $^{31}\text{P}$  NMR spectra were recorded at 25  $^{\circ}$ C on a Varian Mercury 400 MHz spectrometer using deuterated solvents. Tetramethylsilane (TMS) was used as an internal reference (0 ppm) for  $^1\text{H}$  spectra recorded in  $\text{CDCl}_3$  and the residual signal of the solvent (77.16 ppm) for  $^{13}\text{C}$  spectra. Chemical shifts are reported in part per million (ppm) in the d scale, coupling constants (J) in Hz, and multiplicity as follows: s (singlet), d (doublet), t (triplet), q (quadruplet), quint (quintuplet), m (multiplet), and br (broad signal). HPLC analysis and separations were performed using a Waters 2695 Separations Module equipped with a Waters 2998 Photodiode Array Detector. Purification methods: Solvent A: 5%  $\text{CH}_3\text{CN}$  in 100 mM triethylammonium acetate (TEAA) (pH = 7) and solvent B: 70%  $\text{CH}_3\text{CN}$  in 100 mM TEAA (pH = 7). Column: XBridgeTM OST C18 semipreparative column (10  $\times$  50 mm, 2.5 mm). Flow rate: 3 mL/min. Conditions: 10 min of linear gradient from 0% to 30% of B. The pure fractions were combined and evaporated to dryness. The resulting oligomers were analyzed by mass spectrometry (MALDI-TOF), UV/vis spectroscopy, and HPLC as well using the conditions and gradients described above but using the corresponding analytical column (XBridgeTM OST C18 (4.6  $\times$  50 mm, 2.5  $\mu$ m). Flow rate: 1 mL/min). Electrospray ionization mass spectra (ESI-MS) were recorded on a Micromass ZQ instrument with single quadrupole detector coupled to an HPLC, and high-resolution (HR) ESI-MS on an Agilent 1100 LC/MS-TOF instrument (Servei d'Espectrometria de Masses, Universitat de Barcelona). Matrix-assisted laser desorption ionization time-of-flight (MALDI-TOF) mass spectra were recorded on a Voyager-DETMRP spectrometer (Applied Biosystems) in negative mode (2,4,6-trihydroxyacetophenone matrix with ammonium citrate as additive).

**Silanization of Slides.** Si-based wafers were cut into pieces of 2  $\times$  1 cm $^2$  and cleaned with piranha solution ( $\text{H}_2\text{SO}_4$ :30%  $\text{H}_2\text{O}_2$  3:1 v/v) for 1 h at 50  $^{\circ}$ C to remove organic contaminants. *Caution: Piranha solutions react violently with organic materials and should be handled with extreme care.* Then the chip was washed with deionized water and air-dried. To introduce reactive functional groups, the chip was immersed under an argon atmosphere into a solution of the corresponding organosilane 2% in toluene for 2 h at room temperature. For the alkene-functionalized slides, chips were treated with allyltrimethoxysilane (Strategy A); whereas for the thiol-functionalized slides, 3-mercaptopropyl trimethoxysilane (Strategy B) was used. After 2 h, the chip was washed with 2-propanol and air-dried. Finally, the chips were baked for 10 min at 150  $^{\circ}$ C and stored under inert atmosphere.

**Oligonucleotide Immobilization.** Two different strategies based on the use of different silane reagents were assayed for oligonucleotide immobilizations.



**Strategy A.** Silicon-oxide slides were treated following the above-described procedure to obtain the corresponding alkene-functionalized surfaces. To perform this study, oligonucleotide probe A (Table 1), consisting of 5' SH-, 3' Cy5 oligomer of sequence (T)<sub>15</sub>-(CCC GAT TGA CCA GCT AGC ATT) was used to evaluate the efficiency of the platform toward oligonucleotide immobilization. For that, different probe A solutions were prepared and spotted (40 nL) onto the alkene-functionalized surface and exposed to UV-light at 365 nm with a mercury capillary lamp (6 mW/cm<sup>2</sup>, Jelight Irvine, CA, USA) placed at a fixed distance (~0.5 cm) from the slide for 20 min to induce the immobilization. Finally, slides were thoroughly rinsed with PBS-T and water and air-dried. Immobilization results were obtained from the fluorescence signals using the SFR. Measurements were made by accumulation of emitted light by the samples during 15 s with a device gain of 5.

**Strategy B.** Silicon-oxide slides were treated following the above-described procedure to obtain the corresponding thiol-functionalized slides. Thus, oligonucleotide probe H (Table 1), consisting of 5'-alkene-, 3' Cy5 oligomer of sequence TTG ATT ACA GCC GGT GTA CGA CCC T, was used to evaluate the efficiency of the platform toward oligonucleotide immobilization. For that, different probe H solutions were prepared and spotted (40 nL) onto the thiol-functionalized surface and exposed to UV-light at 365 nm for 20 min to induce the immobilization. Finally, slides were thoroughly rinsed with PBS-T and water and air-dried. Immobilization results were obtained from the fluorescence intensity of the spots registered with the SFR.

**Hybridization Assays.** To study the hybridization efficiency on the developed platform, silicon-based slides were functionalized with the appropriate organosilane reactive as described above. Afterward, solutions containing oligonucleotide 5' SH- or alkene-labeled (probes B or I) were spotted (40 nL) onto the functionalized slides creating the microarrays. Then slides were exposed to UV-light at 365 nm (6 mW/cm<sup>2</sup>) for 20 min, washed with water and air-dried. After washing, 50  $\mu$ L of the complementary strand was spread out with a coverslip. After incubation in a slim box for 45 min at 37 °C, the coverslip was gently removed and the chip was washed with PBS-T and deionized water. The fluorescence intensity of the spots was registered with the SFR.

**Detection of Mismatches.** **Strategy A.** To investigate the sensitivity of the system, four oligonucleotide sequences, namely, SH-(T)<sub>15</sub>-(CCC GAT TGA CCA GCT AGC ATT) (probe B, PM), SH-(T)<sub>15</sub>-(CCC GAT TGA CCT GCT AGC ATT) (probe C, MM1), SH-(T)<sub>15</sub>-(CCC GAT TGA TTA GCT AGC ATT) (probe D, MM2), and SH-(T)<sub>15</sub>-CCA TAT TGA CCA GCT ATC ATT) (probe E, MM3) having zero, one, two, and three base mismatches, respectively, were spotted (40 nL/spot, 0.5  $\mu$ M) with a noncontact dispenser onto an alkene-functionalized silicon oxide chip. After immobilization and blocking as described above, the microarray was subjected to hybridization with a labeled oligomer (target A), Cy5-(AAT GCT AGC TGG TCA ATC GGG) in SSC under different conditions for 1 h at 37 °C. After washing and drying, the fluorescence was detected in the SFR.

**Strategy B.** In this case, four alkene-modified oligonucleotide sequences previously synthesized, namely, alkene-(TTG ATT ACA GCC GGT GTA CGA CCC T) (probe I, PM), alkene-(TTG ATT ACA GCC GAT GTA CGA CCC T) (probe J, MM1), alkene-(TTG ATT ACA GCA TGT GTA CGA CCC T) (probe K, MM2), and alkene-(TTG AAA ACA

GCC GGT GTA CGT CCC T) (probe L, MM3) having zero, one, two, and three base mismatches, respectively, were spotted (40 nL/spot, 0.5  $\mu$ M) with a noncontact dispenser onto an thiol-functionalized silicon oxide chip. After immobilization and blocking as described above, the microarray was subjected to hybridization with a labeled oligomer (target B), Cy5-(AGG GTC ACA CCG GCT GTA ATC AAA) in SSC under different conditions for 1 h at 37 °C. After washing and drying, the fluorescence was detected in the SFR.

**Detection of *Escherichia coli*.** Silicon-based slides were functionalized with allyltrimethoxysilane as described above. Then, solutions containing SH-labeled probe F (*E. coli* specific probe) and probe G (negative control probe) were spotted onto the functionalized slides creating the microarrays. Positive and negative controls were included to check the quality of the assay. Afterward, slides were exposed to UV-light at 365 nm for 20 min and subsequently washed and air-dried. Then, Cy5-labeled PCR product solutions (50  $\mu$ L) in hybridization buffer (1 $\times$  SSC) were distributed on the chip. PCR duplexes were first melted by 5 min incubation at 95 °C followed by fast cooling for 1 min on ice. After incubating 1 h at 37 °C, the slides were washed with PBS-T, rinsed with deionized water, and air-dried.

**Synthesis of Monoallyl-tetraethylene glycol Phosphoramidite 3-[2-[2-[2-(allyloxyethoxy)ethoxy]-ethoxy]-ethoxy-(diisopropylamino)phosphanyl]-oxapropan-enitrile.** Monoallyl-tetraethylene glycol (150 mg; 0.640 mmol) was previously dissolved in anhydrous acetonitrile (3  $\times$  10 mL). The solvent was evaporated under reduced pressure and the resulting alcohol was dried in vacuum for one hour. The alcohol was then dissolved in anhydrous dichloromethane (2 mL) and DIEA (2.0 equiv) was added dropwise at room temperature. The solution was cooled at 0 °C and phosphine reagent (1.1 equiv) was carefully added dropwise. The reaction was stirred 5 min at 0 °C and 1 h at room temperature and monitored by TLC. Dichloromethane was added (10 mL) and organic layer was washed with a NaHCO<sub>3</sub> 0.5 M solution (1  $\times$  5 mL) and brine (1  $\times$  5 mL). Finally, solvent was evaporated and crude was purified by flash chromatography (Hex/AcOEt 1% to 20. <sup>1</sup>H NMR (400 MHz, CDCl<sub>3</sub>)  $\delta$  5.87 (m, 1H), 5.20 (m, 2H), 4.00 (t, *J* = 7.1 Hz; 2H), 3.97 (t, *J* = 7.0 Hz; 2H), 3.81 (m, 2H), 3.62 (m, 14H), 3.58 (m, 4H), 2.64 (m, 2H), 1.16 (d, *J* = 7.02 Hz; 6H), 1.14 (d, *J* = 7.01 Hz; 6H). <sup>13</sup>C NMR (100 MHz, CDCl<sub>3</sub>)  $\delta$  134.7, 117.0, 72.2, 71.1, 70.5, 69.3, 62.6, 58.4, 42.9, 24.6, 20.3. <sup>31</sup>P NMR (162 MHz, CDCl<sub>3</sub>)  $\delta$  149.9. HRMS (ESI +): *m/z* calcd for C<sub>20</sub>H<sub>39</sub>N<sub>2</sub>O<sub>6</sub>P ([M+H]<sup>+</sup>) 435.2618; found 435.2617.

## ■ ASSOCIATED CONTENT

### Supporting Information

HPLC analysis and mass spectra of designed oligonucleotide probes, water contact angle measurements, surface characterization (XPS, AFM and IRRAS figures), oligonucleotide calibration curves, DPI measurements. This material is available free of charge via the Internet at <http://pubs.acs.org>.

## ■ AUTHOR INFORMATION

### Corresponding Author

\*Phone: 34-963873415; fax: 34-963879349; E-mail: [amaqueira@quim.upv.es](mailto:amaqueira@quim.upv.es).

### Notes

The authors declare no competing financial interest.



## ■ ACKNOWLEDGMENTS

Financial support from Ministerio de Ciencia e Innovación (CTQ2010-15943) and Generalitat Valenciana (PROMETEO/2010/008 and ACOMP/2012/158) is acknowledged. The authors are grateful to the Servei d'Espectrometria de Masses of the Universitat de Barcelona for the spectroscopic facilities.

## ■ REFERENCES

- (1) Baldi, P., and Hatfield, G. W. (2011) *DNA microarrays and gene expression: from experiments to data analysis and modeling*, pp 7–15, Cambridge University Press, Cambridge.
- (2) Sassolas, A., Leca-Bouvier, B. D., and Blum, L. J. (2008) DNA biosensors and microarrays. *Chem. Rev.* 108, 109–139.
- (3) Samanta, D., and Sarkar, A. (2011) Immobilization of bio-molecules on self-assembled monolayers: methods and sensor applications. *Chem. Soc. Rev.* 40, 2567–2592.
- (4) Crick, C. R., and Parkin, I. P. (2010) Preparation and characterisation of super-hydrophobic surfaces. *Chem.—Eur. J.* 16, 3568–3588.
- (5) Shylesh, S., Schunemann, V., and Thiel, W. R. (2010) Magnetically separable nanocatalysts: bridges between homogeneous and heterogeneous catalysis. *Angew. Chem., Int. Ed.* 49, 3428–3459.
- (6) Valentini, L., Cardinali, M., and Kenny, J. M. (2010) Selective deposition of semiconducting single-walled carbon nanotubes onto amino-silane modified indium tin-oxide surface for the development of poly(3-hexylthiophene)/carbon-nanotube photovoltaic heterojunctions. *Carbon* 48, 861–867.
- (7) LeMieux, M. C., Roberts, M., Barman, S., Jin, Y. W., Kim, J. M., and Bao, Z. N. (2008) Self-sorted, aligned nanotube networks for thin-film transistors. *Science* 321, 101–104.
- (8) Melde, B. J., Johnson, B. J., and Charles, P. T. (2008) Mesoporous silicate materials in sensing. *Sensors* 8, S202–S228.
- (9) Dugas, V., Demesmay, C., Chevolut, Y., and Souteyrand, E. (2010) *Use of organosilanes in biosensors*, Nova Science Publishing Inc., New York.
- (10) Mrksich, M., and Whitesides, G. M. (1995) Patterning self-assembled monolayers using microcontact printing - a new technology for biosensors. *Trends Biotechnol.* 13, 228–235.
- (11) Singhvi, R., Kumar, A., Lopez, G. P., Stephanopoulos, G. N., Wang, D. I., Whitesides, G. M., and Ingber, D. E. (1994) Engineering cell shape and function. *Science* 264, 696–698.
- (12) Place, E. S., Evans, N. D., and Stevens, M. M. (2009) Complexity in biomaterials for tissue engineering. *Nat. Mater.* 8, 457–470.
- (13) Schulz, C., Nowak, S., Frohlich, R., and Ravoo, B. J. (2012) Covalent layer-by-layer assembly of redox active molecular multilayers on silicon (100) by photochemical thiol-ene chemistry. *Small* 8, 569–577.
- (14) Chen, Y. X., Triola, G., and Waldmann, H. (2011) Bioorthogonal Chemistry for site-specific labeling of surface immobilization of proteins. *Acc. Chem. Res.* 44, 762–773.
- (15) Dondoni, A. (2008) The emergence of thiol-ene coupling as a click process for materials and bioorganic chemistry. *Angew. Chem., Int. Ed.* 47, 8995–8997.
- (16) Hoyle, C. E., and Bowman, C. N. (2010) Thiol-ene click chemistry. *Angew. Chem., Int. Ed.* 49, 1540–1573.
- (17) Kempe, K., Krieg, A., Becer, C. R., and Schubert, U. S. (2012) “Clicking” on/with polymers: a rapidly expanding field for the straightforward preparation of novel macromolecular architectures. *Chem. Soc. Rev.* 41, 176–191.
- (18) Lowe, A. (2010) Thiol-ene “click” reactions and recent applications in polymer and materials synthesis. *Polym. Chem.* 1, 17–36.
- (19) Jonkheijm, P., Weinrich, D., Köhn, M., Engelkamp, H., Christianen, P. C. M., Kuhlmann, J., Maan, J. C., Nüsse, D., Schroeder, H., Wacker, R., Breinbauer, R., Niemeyer, C. M., and Waldmann, H. (2008) Photochemical surface patterning by the thiol-ene reaction. *Angew. Chem., Int. Ed.* 47, 4421–4424.
- (20) Bertin, A., and Schlaad, H. (2009) Mild and versatile (bio-)functionalization of glass surfaces via thiol-ene photochemistry. *Chem. Mater.* 21, 5698–5700.
- (21) Gupta, N., Lin, B. F., Campos, L. M., Dimitriou, M. D., Hikita, T. S., Treat, N. D., Tirrell, M. V., Clegg, D. O., Kramer, E. J., and Hawker, C. J. (2010) A versatile approach to high-throughput microarrays using thiol-ene chemistry. *Nat. Chem.* 2, 138–145.
- (22) Weinrich, D., Lin, P.-C., Jonkheijm, P., Nguyen, U. T. T., Schröder, H., Niemeyer, C. M., Alexandrov, K., Goody, R., and Waldmann, H. (2010) Oriented immobilization of farnesylated proteins by the thiol-ene reaction. *Angew. Chem., Int. Ed.* 49, 1252–1257.
- (23) Madan, N., Terry, A., Harb, J., Davis, R. C., Schlaad, H., and Linford, M. R. (2011) Thiol-ene-thiol photofunctionalization of thiolated monolayers with polybutadiene and functional thiols, including thiolated DNA. *J. Phys. Chem. C* 115, 229318–22938.
- (24) Wendeln, C., Rinnen, S., Schulz, C., Kaufmann, T., Arlinghaus, H. F., and Ravoo, B. J. (2012) Rapid preparation of multifunctional surfaces for orthogonal ligation by microcontact chemistry. *Chem.—Eur. J.* 18, 5880–5888.
- (25) Wasserberg, D., Steentjes, T., Stopel, M. H. W., Huskens, J., Blum, C., Subramaniam, V., and Jonkheijm, P. (2012) Patterning perylenes on surfaces using thiol-ene chemistry. *J. Mater. Chem.* 22, 16606–16610.
- (26) Escorihuela, J., Bañuls, M. J., Puchades, R., and Maquieira, A. (2012) DNA microarrays on silicon surfaces through thiol-ene chemistry. *Chem. Commun.* 48, 2116–2118.
- (27) Lafleur, J. P., Kwapiszewski, R., Jensen, T. G., and Kutter, J. P. (2013) Rapid photochemical surface patterning of proteins in thiol-ene based microfluidic devices. *Analyst* 138, 845–849.
- (28) Oberleitner, B., Dellinger, A., Déforet, M., Galtayries, A., Castanet, A.-S., and Semetey, V. (2013) A facile and versatile approach to design self-assembled monolayers on glass using thiol-ene chemistry. *Chem. Commun.* 49, 1615–1617.
- (29) Gong, P., Harbers, G. M., and Grainger, D. W. (2006) Multi-technique comparison of immobilized and hybridized oligonucleotide surface density on commercial amine-reactive microarray slides. *Anal. Chem.* 78, 2342–2351.
- (30) Li, Y., Wang, Z., Ou, L. M. L., and Yu, H.-Z. (2007) DNA detection on plastic: surface activation protocol to convert polycarbonate substrates to biochip platforms. *Anal. Chem.* 79, 426–433.
- (31) Kim, H. J., Yoon, J. H., and Yoon, S. (2010) Photooxidative coupling of thiophenol derivatives to disulfides. *J. Phys. Chem. A* 114, 12010–12015.
- (32) Tamarit-López, J., Morais, S., Puchades, R., and Maquieira, A. (2011) Oxygen plasma treated interactive polycarbonate DNA microarraying platform. *Bioconjugate Chem.* 22, 2573–2580.
- (33) Li, Y., and Zuilhof, H. (2012) Photochemical grafting and patterning of organic monolayers on indium tin oxide substrates. *Langmuir* 28, 5350–5359.
- (34) Wasserberg, D., Nicosia, C., Tromp, E. E., Subramaniam, V., Huskens, J., and Jonkheijm, P. (2013) Oriented protein immobilization using covalent and noncovalent chemistry on a thiol-reactive self-reporting surface. *J. Am. Chem. Soc.* 135, 3104–3111.
- (35) Weitekamp, R. A., Atwater, H. A., and Grubbs, R. H. (2013) Photolithographic olefin metathesis polymerization. *J. Am. Chem. Soc.* 135, 16817–16820.
- (36) Escorihuela, J., Bañuls, M. J., Puchades, R., and Maquieira, A. (2012) Development of oligonucleotide microarrays onto si-based surfaces via thioether linkage mediated by UV irradiation. *Bioconjugate Chem.* 23, 2121–2128.
- (37) Ham, H. O., Liu, Z., Lau, K. H. A., and Messersmith, P. B. (2011) Facile DNA immobilization on surfaces through a catechol-amine polymer. *Angew. Chem., Int. Ed.* 50, 732–736.
- (38) Caipa Campos, M. A., Paulusse, J. M. J., and Zuilhof, H. (2010) Functional monolayers on oxide-free silicon surfaces via thiol-ene click chemistry. *Chem. Commun.* 46, 5512–5214.

- (39) Graf, N., Gross, T., Wirth, T., Weigel, W., and Unger, W. (2009) Application of XPS and ToF-SIMS for surface chemical analysis of DNA microarrays and their substrates. *Anal. Bioanal. Chem.* 393, 1907–1912.
- (40) Lee, C.-Y., Gong, P., Harbers, G. M., Grainger, D. W., Castner, D. G., and Gamble, L. J. (2006) Surface coverage and structure of mixed DNA/alkylthiol monolayers on gold: characterization by XPS, NEXAFS, and fluorescence intensity measurements. *Anal. Chem.* 78, 3316–3325.
- (41) Rouillat, M. H., Dugas, V., Martin, J. R., and Phaner-Goutorbe, M. (2005) Characterization of DNA chips on the molecular scale before and after hybridization with an atomic force microscope. *Appl. Surf. Sci.* 252, 1765–1771.
- (42) Phaner-Goutorbe, M., Dugas, V., Chevolot, Y., and Souteyrand, E. (2011) Silanization of silica and glass slides for DNA microarrays by impregnation and gas phase protocols: A comparative study. *Mater. Sci. Eng., C* 31, 384–390.
- (43) Wang, C., Jia, X.-M., Jiang, C., Zhuang, G.-N., Yan, Q., and Xiao, S.-J. (2012) DNA microarray fabricated on poly(acrylic acid) brushes-coated porous silicon by in situ rolling circle amplification. *Analyst* 137, 4539–4545.
- (44) Bammler, T., Beyer, R. P., Bhattacharya, S., Boorman, G. A., Boyles, A., Bradford, B. U., Bumgarner, R. E., Bushel, P. R., Chaturvedi, K., Choi, D., Cunningham, M. L., Dengs, S., Dressman, H. K., Fannin, R. D., Farun, F. M., Freedman, J. H., Fry, R. C., Harper, A., Humble, M. C., Hurban, P., Kavanagh, T. J., Kaufmann, W. K., Kerr, K. F., Jing, L., Lapidus, J. A., Lasarev, M. R., Li, J., Li, Y. J., Lobenhofer, E. K., Lu, X., Malek, R. L., Milton, S., Nagalla, S. R., O'Malley, J. P., Palmer, V. S., Pattee, P., Paules, R. S., Perou, C. M., Phillips, K., Qin, L. X., Qiu, Y., Quigley, S. D., Rodland, M., Rusyn, I., Samson, L. D., Schwartz, D. A., Shi, Y., Shin, J. L., Sieber, S. O., Slifer, S., Speer, M. C., Spencer, P. S., Sproles, D. I., Swenberg, J. A., Suk, W. A., Sullivan, R. C., Tian, R., Tennant, R. W., Todd, S. A., Tucker, C. J., Van Houten, B., Weis, B. K., Xuan, S., and Zarbl, H. (2005) Standardizing global gene expression analysis between laboratories and across platforms. *Nat. Methods* 2, 351–356.
- (45) Banoub, J. H., Newton, R. P., Esmans, E., Ewing, D. F., and Mackenzie, G. (2005) Recent developments in mass spectrometry for the characterization of nucleosides, nucleotides, oligonucleotides, and nucleic acids. *Chem. Rev.* 105, 1869–1916.
- (46) Wang, K., Tang, Z., Yang, C. J., Kim, Y., Fang, X., Li, W., Wu, Y., Medley, C. D., Cao, Z., Li, J., Colon, P., Lin, H., and Tan, W. (2009) Molecular engineering of DNA: molecular beacons. *Angew. Chem., Int. Ed.* 48, 856–870.
- (47) Escorihuela, J., Bañuls, M. J., García-Castelló, J., Toccafondo, V., García-Rupérez, J., Puchades, R., and Maquieira, A. (2012) Chemical silicon surface modification and bioreceptor attachment to develop competitive integrated photonic biosensors. *Anal. Bioanal. Chem.* 404, 2831–2840.
- (48) Xu, P., Huang, F., and Liang, H. (2013) Real-time study of a DNA strand displacement reaction using dual polarization interferometry. *Biosens. Bioelectron.* 41, 505–510.
- (49) López-Paz, J. L., González-Martínez, M. A., Escorihuela, J., Bañuls, M. J., Puchades, R., and Maquieira, A. (2014) Direct and label-free monitoring oligonucleotide immobilization, non-specific binding and DNA biorecognition. *Sens. Actuator, B* 192, 221–228.
- (50) Elhadj, S., Singh, G., and Saraf, R. F. (2004) Optical properties of an immobilized DNA monolayer from 255 to 700 nm. *Langmuir* 20, 5539–5543.
- (51) Mira, D., Llorente, R., Morais, S., Puchades, R., Maquieira, A., and Martí, J. (2004) High throughput screening of surface-enhanced fluorescence on industrial standard digital recording media. *Proc. SPIE* 5617, 364–373.